Light-Emitting Illumination and Field Emission Device of Potassium Hydroxide-Doped Electrochemically Reduced Graphene Oxide

Ching-Tsang Chang, Yi-Tsung Chang, *Member, IEEE*, Yun-Jhong Chih, Yu-Hao Lee, Chun-Hu Chen, Lung-Chien Chen, and Jau-Je Wu

***Abstract*— This paper presents a parallel plate-type field emission device of potassium hydroxide-doped electrochemically reduced graphene oxide (GO) manufactured using highly oriented pyrolytic graphite through electrochemical exfoliation. The material properties of the GO were tested through Raman spectroscopy, X-ray diffraction, and X-ray photoelectron spectroscopy. The optimal electron emission characteristics of the device were as follows: turn-on field $= 2.03$ V/μm, field emission current $= 16.4$ μA, and field emission enhancement factor $= 8377$. At an emission peak wavelength of 563.7 nm, the optimal device had a light flux of 4.21 lumens and an illumination of 140.3 lux. These properties can be utilized in various optoelectronic devices, such as nanoelectronics devices, sensors, electrochemical systems, and energy storage devices.**

***Index Terms*— Field emission, graphene oxide (GO), highly oriented pyrolytic graphite (HOPG), light-emitting illumination.**

I. Introduction

AFTER being theorized for years, graphene was finally isolated and characterized in 2004. Graphene has since been extensively studied, and graphene-based products, such as energy storage devices [1], nanoelectronics products [2], electrochemical systems [3], and sensors [4], have been developed. Graphene is an advanced nanomaterial of great academic and industrial interest because of its unique physical graphene oxide (GO) is usually produced through the Hummer method [8] and through other chemical syntheses [9]. Graphite oxide sheets, simply called GO, are products of the chemical oxidation and exfoliation of graphite powder. GO sheets are single-atomic-layer sheets spanning tens of micrometers in their lateral dimension, bridging across the typical length scales investigated in chemistry and materials science [10]. Field emission refers to the process wherein electrons tunnel through a potential-energy barrier at the solid–vacuum interface and then escape into the vacuum under an external electrostatic field and to the process wherein electrons are emitted from the surface of the material when an external electric field is applied [11], [12]. In recent years, the field emission phenomenon of graphene [13] has received much

TABLE I
Insert Voltage and Solution of All Samples

Samples	Insert Voltage (V)	H2SO4 (M)	KOH (M)
A	1	0.48	0
B	1	0.96	0
C	2.5	0.48	0
D	2.5	0.96	0
E	1	0.48	0.487
F	1	0.96	0.487
G	2.5	0.48	0.487
H	2.5	0.96	0.487

TABLE II
Raman Analysis Information for All Samples

Samples	I_D/I_G	2D band FWHM (cm^{-1})
A	4.12	96.29
B	2.56	107.74
C	2.19	98.17
D	2.13	95.9
E	1.23	88.7
F	1.08	97.6
G	1.38	96.73
H	1.48	111.77

Manuscript received December 1, 2016; revised February 9, 2017; accepted February 28, 2017. Date of current version April 19, 2017. This work was supported in part by the Department of Electrical Engineering, National Sun Yat-sen University Prof. T.-S. Horng (Fellow, IEEE) and in part by the National Science Council of China, Taiwan, under Contract NSC 103-ET-E-110-002-ET and Contract MOST 103-2221-E-110-036. The review of this paper was arranged by Editor E. G. Johnson.

C.-T. Chang, Y.-J. Chih, and Y.-H. Lee are with the Department of Electrical Engineering, National Sun Yat-sen University, Kaohsiung 80424, Taiwan (e-mail: ching1105@outlook.com; john64018@yahoo.com.tw; jazzwesley@gmail.com).

Y.-T. Chang is with the Department of Electrical Engineering, National Sun Yat-sen University, Kaohsiung 80424, Taiwan, and also with the Research and Development Affairs Office, Taipei College of Maritime Technology, New Taipei 25172, Taiwan (e-mail: ytchang@mail.ee.nsysu.ntu.edu.tw).

C.-H. Chen is with the Department of Chemistry, National Sun Yat-sen University, Kaohsiung 80424, Taiwan (e-mail: chunhu.chen@mail.nsysu.edu.tw).

L.-C. Chen is with the Department of Electro-Optical Engineering, National Taipei University of Technology, Taipei 10608, Taiwan (e-mail: ocean@ntut.edu.tw).

J.-J Wu is with the Research and Development Affairs Office, Taipei college of maritime technology, New Taipei 25172, Taiwan (e-mail: jaujewu@mail.tcmt.edu.tw).

Color versions of one or more of the figures in this paper are available online at http://ieeexplore.ieee.org.

Digital Object Identifier 10.1109/TED.2017.2678020

0018-9383 © 2017 IEEE. Personal use is permitted, but republication/redistribution requires IEEE permission.
See http://www.ieee.org/publications_standards/publications/rights/index.html for more information.

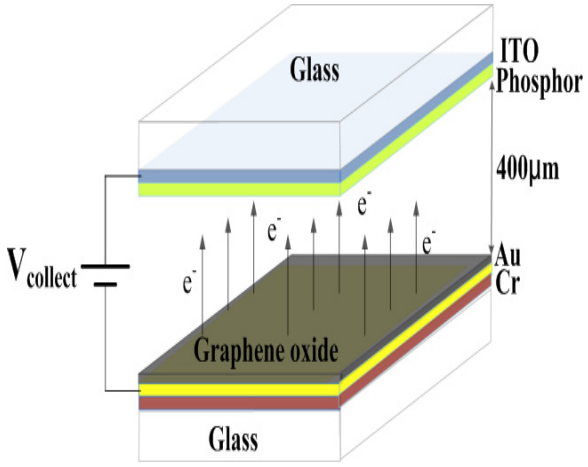

Fig. 1. Field emission light-emitting device structure.

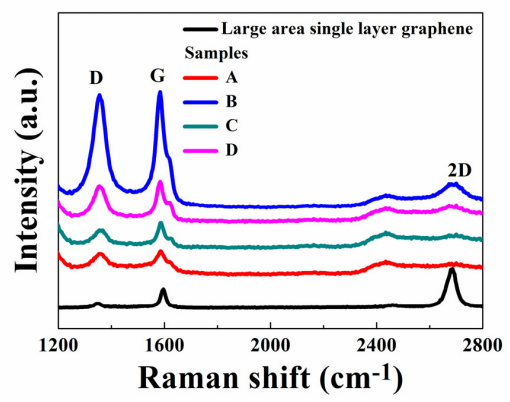

(a)

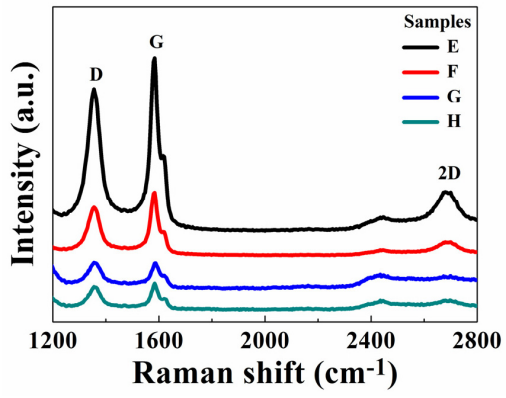

(b)

Fig. 2. Raman spectra for (a) pristine GO and (b) electrochemically r-GO.

academic attention owing to graphene's favorable electrical conductivity, electron mobility, and aspect ratio. In this paper, GO was produced through electrochemical exfoliation, a simple and convenient method. In addition, a parallel plate-type field emission device of GO was fabricated. GO was drop coated [14] on substrates to manufacture cathodes for a field emission device.

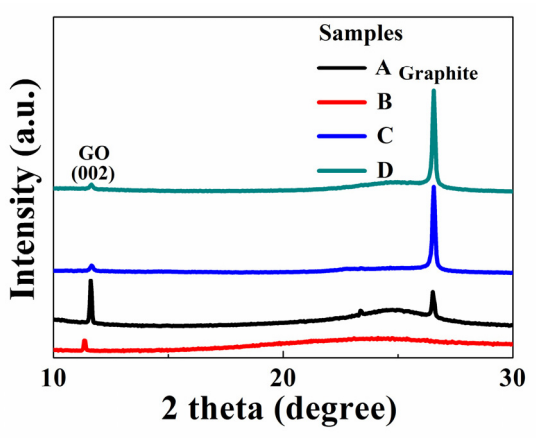

(a)

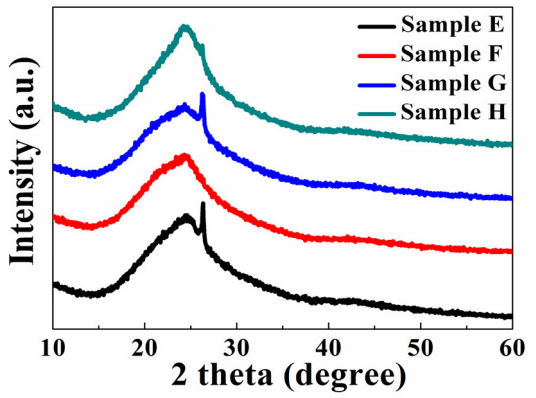

(b)

Fig. 3. XRD patterns for (a) pristine GO and (b) electrochemical r-GO.

II. Experiment

A. Producing GO and Reduced Products

A highly oriented pyrolytic graphite (HOPG) was first electrolyzed using a mixture of 0.48–0.96 M sulfuric acid (98%), 0.487 M potassium hydroxide, and 100-mL deionized water. The HOPG was attached to a platinum wire using a copper tape and was used as the anode, and another platinum wire was used as the cathode. The power supply in the experiment was set to 2.5 V as the insert voltage for 5 min; the bias was then changed to 12 V for 15 min [15], [16]. Subsequently, GO was collected through filtration and preserved in N,N-dimethylformamide solution. Tables I and II present the properties of the GO samples.

Reduced GO (r-GO) used in this experiment was the same as that discussed in the previous paragraph; the insert voltage was set as 1–2.5 V, and 0.487 M KOH was added to the original electrolyte in order to reduce the number of graphene defects [17].

B. Material Analysis

All samples were characterized through Raman spectroscopy (Witec Confocal Raman Microscope Alpha 300R), X-ray diffraction (XRD; Bruker D2 Phaser), and X-ray photoelectron spectroscopy (XPS; JEOL JPS-9010 MX).

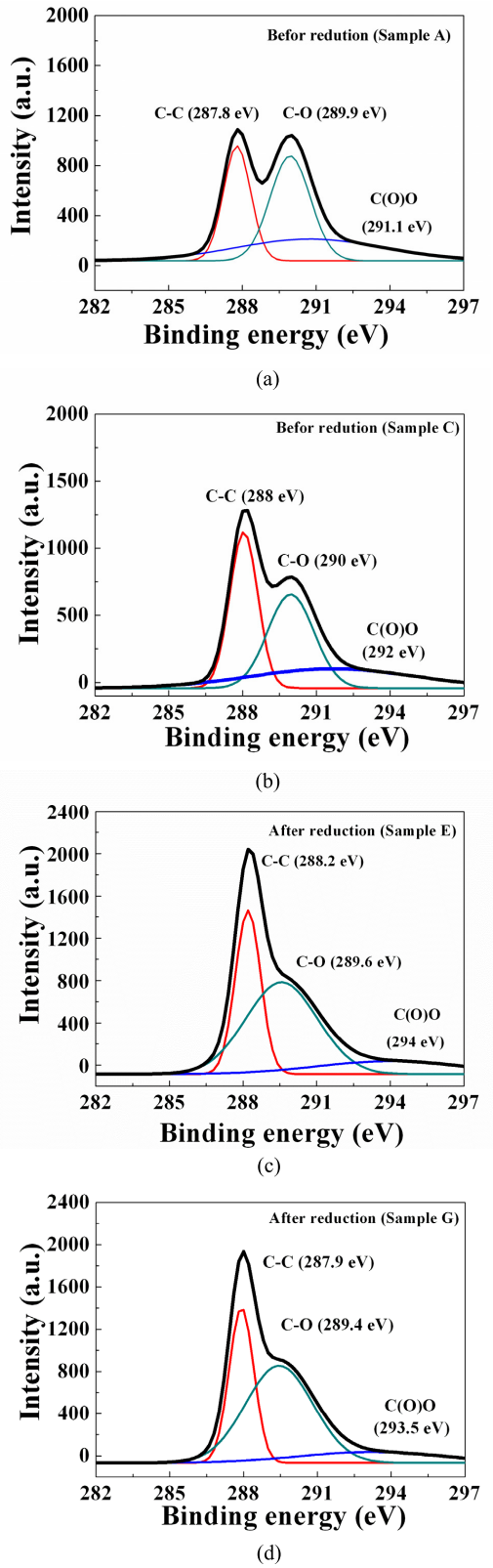

Fig. 4. XPS spectra for (a) and (b) are samples A and C before reduction, and (c) and (d) are samples E and G after reduction.

Raman spectroscopy revealed the characteristic bands of graphene (e.g., D, G, and 2-D bands). The crystal structure of GO was characterized through XRD, and the constituent elements, electronic and chemical states, and chemical bonding of

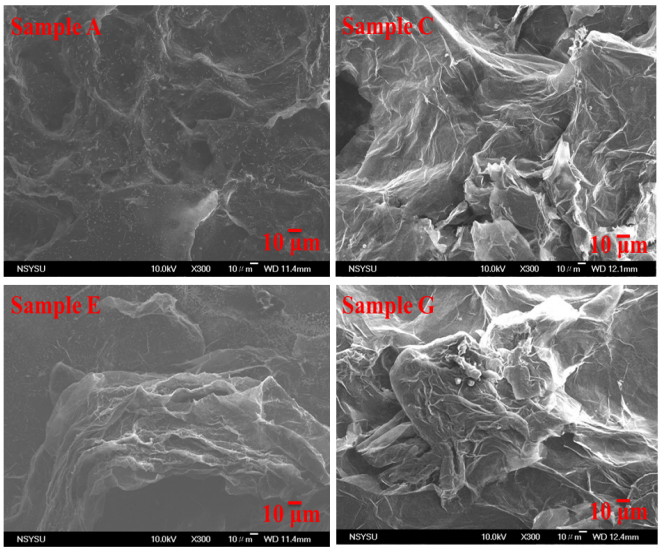

Fig. 5. SEM images of GO (samples A and C) and r-GO (samples E and G).

GO were examined through XPS. All characterizations verified improvement in the material properties.

C. Field Emission Measurement

The experiment on the field emission of electrons was based on Fowler–Nordeim (F–N) theory [11], [18]

$$I = A\frac{a\cdot(\beta E)^2}{\phi}\cdot\exp\left(\frac{-b\phi^{1.5}}{\beta E}\right) \tag{1}$$

where A is the emission area, φ is the work function, β is the field enhancement factor, and a and b are constants ($a = 1.54\times10^{-6}$ A·eV·V^{-2} and $b = 6.83\times10^{7}$ eV$^{-1.5}$·V·cm^{-1}). Fig. 1 shows the structure of the fabricated device; the gold and chrome electrical contacts were formed through electron-beam evaporation on a glass substrate. GO was drop coated [14] on the substrate as the cathode. A 150-nm-thick indium tin oxide (ITO) layer coated on the substrate through sputter deposition served as the anode. The field emission electron experiment was performed using a parallel-plate setup in a vacuum chamber (Edwards RV12; 1.5×10^{-3} torr). The anode–cathode distance (d) was approximately 400 μm, and the measured emission area was 1×1 cm^2. A high-voltage power supply (YSTC HVPS) delivered a stable voltage to the anode, and the voltage was swept from 0 to 2000 V in steps of 10 V. Field emission light-emitting illumination and spectral measurements were performed in the same manner as were the electrical measurements; however, instead of sputter-deposited ITO, a spin-coated phosphor layer (phosphor: methanol = 1:5 by weight, 600 rpm for 40 s) was used as the anode.

III. Results and Discussion

A. Raman Analysis

Raman spectroscopy is a powerful nondestructive method for characterizing carbonaceous materials, especially for identifying the ordered and disordered crystal structures of carbon.

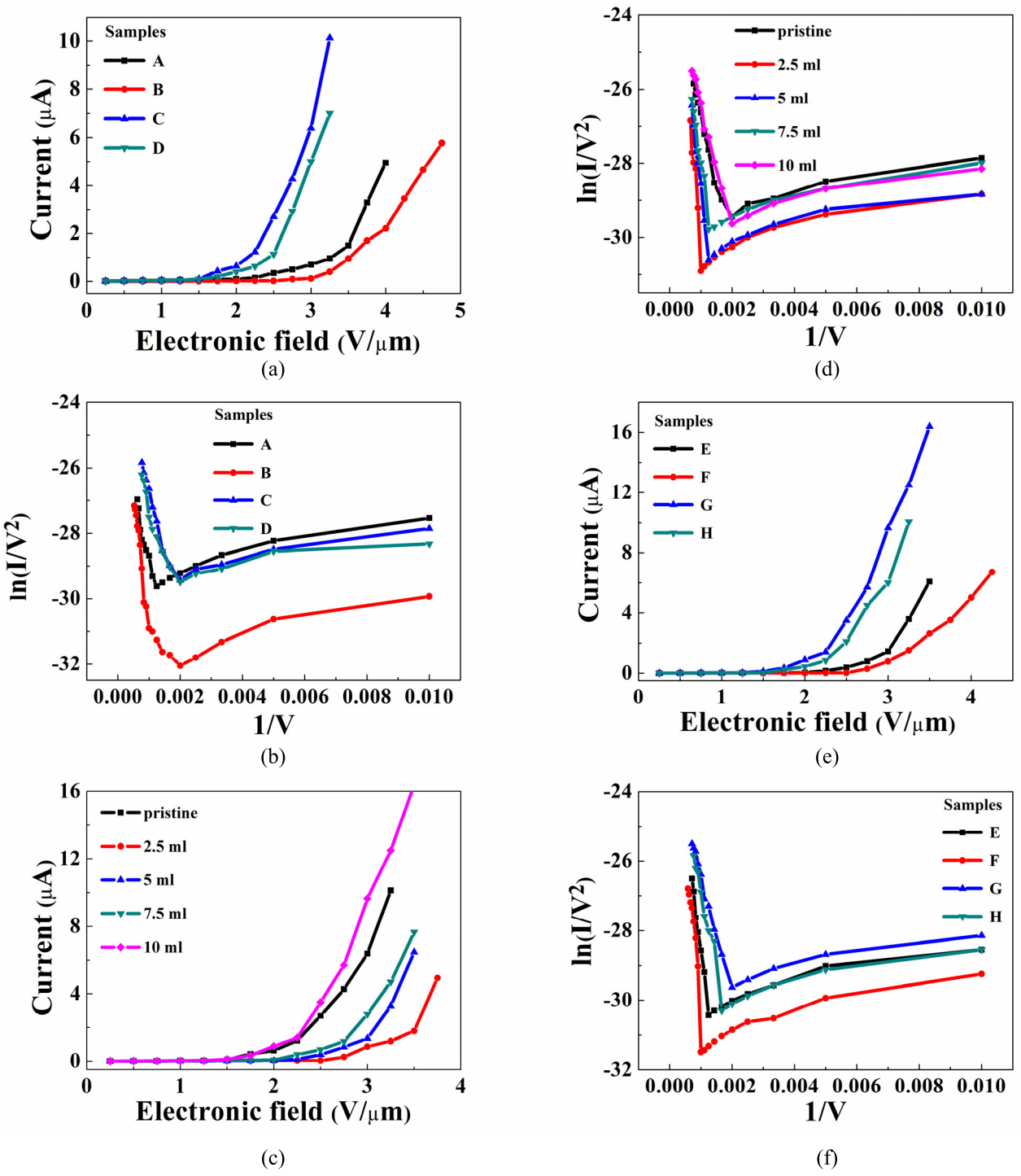

Fig. 6. *I–V* curve and ln(I/V^2) versus 1/V plot of F–N equation for (a) and (b) pristine GO and (c) and (d) samples with different potassium hydroxide contents. (e) and (f) Samples with the optimal potassium hydroxide content.

The significant structural changes that occur during the functionalization of GO are reflected in its Raman spectra [19]. Raman shifts were observed in the *D*, *G*, and 2-D bands, which shifted by 1355, 1584, and 2690 cm^{-1} on average, respectively (Fig. 2) [20], [21]. The *D*-band intensity is affected by the number of defects, and others with higher intensity are attributable to the fast electrochemical preparation. The *G*-band is a characteristic marker of the graphite structure and reflects the vibration of the sp^2 C = C bonding: the more the sp^2 bonding, the higher the strength of the *G*-band. The I_D/I_G data evidence that r-GO has substantially fewer defects than does pristine GO [Table II and Fig. 2(b)]. Samples C and G exhibited the highest quality.

B. XRD Analysis

XRD is a simple method for investigating the structure of a crystalline material, such as graphene. The XRD angles of exfoliated GO and electrochemically r-GO are 10.4° and 26.5°,

respectively [22]. The XRD angles of the GO samples before and after reduction were 11.3°–11.6° and 24.3°, respectively (Fig. 3); the slight shift in the angle of the reduced sample is indicative of its higher purity. The diffraction peak of residual pristine graphite was observed at 26.5° [22].

C. XPS Analysis

XPS [23] is one of the most commonly used methods for determining the relative amounts of carbon, oxygen, and functional groups in GO and is more accurate than the elemental analysis in measuring carbon and oxygen content [24], [25]. XPS revealed that reduction reduces the strength of the chemical bonds of oxygen atoms (Fig. 4); the slight shift in the bonding energy is caused by the retarding effect of the glass substrate [26]. The C1s XPS spectra of GO (samples A and C) and r-GO (samples E and G) exhibited three distinct peaks at 287.7, 289.6, and 292.1 eV, and 287.7, 289.3, and 293.2 eV, respectively, corresponding to the C–C (aromatic rings), C–O (epoxy and alkoxy), and C(O)O groups, proving that the samples are close in quality to pure graphene [27], [28].

D. Scanning Electron Microscopy Analysis

The nanostructure of the samples was examined through scanning electron microscopy (SEM). Fig. 5 presents the morphology of the GO (samples A and C) and r-GO (samples E and G) samples. Samples C and G exhibited a sharp and wrinkly structure and yielded relatively high field emission performance than did the other samples [29], [30].

E. Field Emission, Light Flux, and Illumination of the Fabricated Device

Fig. 6(a) shows the four field emission devices composed of pristine GO samples A–D. The turn-ON fields of samples A–D were 3.26, 3.51, 2.15, and 2.43 V/μm, respectively, and their maximum field emission current levels were 4.95, 5.8, 10.1, and 6.9 μA, respectively. Thus, sample C exhibited the most favorable field emission performance. Fig. 6(e) presents the I–V curves for samples E–H. The turn-ON fields of samples E–H were 2.82, 3.05, 2.03, and 2.27 V/μm, respectively, and their maximum field emission current were 6.1, 6.7, 16.4, and 10 μA, respectively. Thus, of samples E–H, sample G exhibited the most favorable field emission properties.

Fig. 6(b) plots the $\ln(I/V^2)$ versus $1/V$ curve [11] for samples A–D. As evident, F–N tunneling is the dominant field emission current transport mechanism. The slope of the opening upward curve in Fig. 6(b) was calculated. The β values of the four samples were 3404, 4836, 8174, and 5810. Fig. 6(f) shows the F–N curve for samples E–H, indicating their β values to be 3699, 5333, 8377, and 6164.8, respectively.

Sample C exhibited the most favorable field emission properties; its turn-ON field and β were 2.15 V/μm and 8174, respectively. Therefore, to determine the doping concentration that yielded the highest field emission efficiency, potassium hydroxide-doped GO samples were prepared by doping the samples using 2.5, 5, 7.5, and 10 mL of potassium hydroxide in 0.48 M sulfuric acid, because adding potassium hydroxide can increase the density of edge defects [31], which in turn improves device efficiency [18]. The turn-ON fields of samples thus prepared were 2.15, 3.1, 2.8, 2.65, and 2.03 V/m [Fig. 6(c)], and their β values were 3699, 5333, 8377, and 6164 [Fig. 6(d)]. Clearly, the optimal performance was realized when doping using 10 mL of potassium hydroxide.

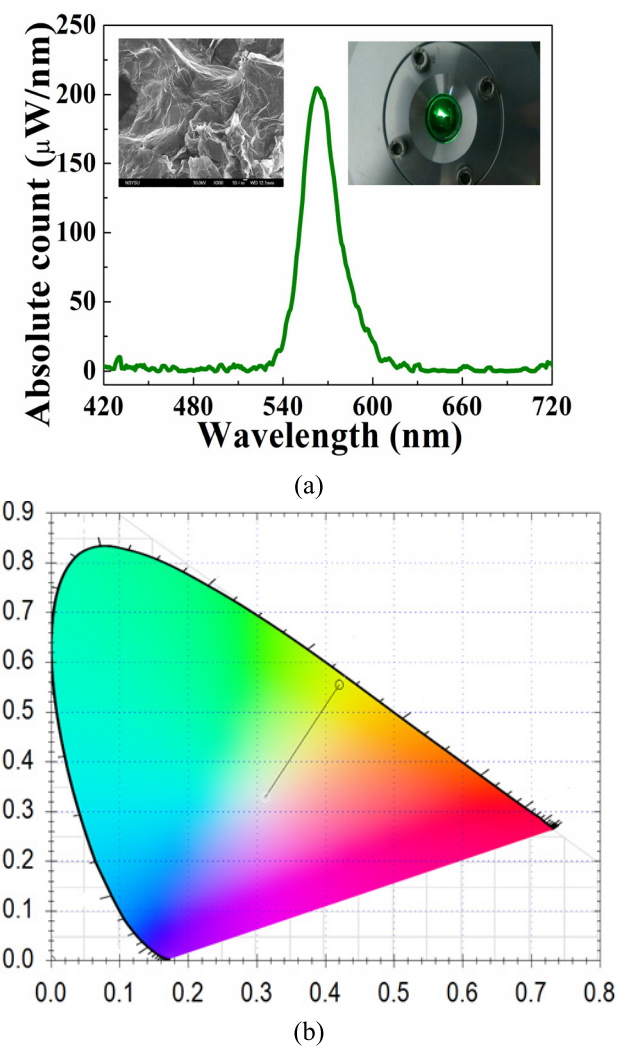

Fig. 7. Optimal device performance. (a) Light wavelength and intensity. (b) CIE chromaticity diagram.

When 0.487 M sulfuric acid and 10 mL of potassium hydroxide was added, the field emission efficiency of sample G improved: its turn-ON field and β were 2.03 V/μm and 8377, respectively (Fig. 6). As shown in Fig. 7, sample G exhibited the highest performance among all devices; at a peak wavelength of 563.7 nm, its light flux was 4.21 lumens and illumination was 140.3 lux.

IV. Conclusion

This paper elucidated the effects of the preparation conditions of GO on its field emission characteristics. Addition of 0.487 M potassium hydroxide reduced the turn-ON field from 2.15 to 2.03 V/μm, increased the field emission current to 16.4 μA, and increased β from 8174 to 8377; at an emission peak, wavelength of 563.7 nm, a light flux of 4.21 lumens, and illumination of 140.3 lux were realized, confirming that GO

with potassium hydroxide exhibits the optimal field emission efficiency. This material can be utilized in large-area flat-panel displays and graphene-based light-emitting devices.

REFERENCES

[1] T. Y. Kim *et al.*, "High-Performance supercapacitors based on poly(ionic liquid)-modified graphene electrodes," *ACS Nano*, vol. 5, no. 1, pp. 436–442, Dec. 2010.

[2] Z. Wei *et al.*, "Nanoscale tunable reduction of graphene oxide for graphene electronics," *Science*, vol. 328, no. 5984, pp. 1373–1376, Jun. 2010.

[3] V. N. Medhekar, A. Ramasubramaniam, S. R. Ruoff, and B. V. Shenoy, "Hydrogen bond networks in graphene oxide composite paper: Structure and mechanical properties," *ACS Nano*, vol. 4, no. 4, pp. 2300–2306, Apr. 2010.

[4] T. Jeremy Robinson, F. Keith Perkins, S. Eric Snow, Z. Wei, and E. Paul Sheehan, "Reduced graphene oxide molecular sensors," *Nano Lett.*, vol. 8, no. 10, pp. 3137–3140, Sep. 2008.

[5] K. I. Bolotin *et al.*, "Ultrahigh electron mobility in suspended graphene," *Solid State Commun.*, vol. 146, pp. 351–355, Jun. 2008.

[6] A. A. Balandin *et al.*, "Superior thermal conductivity of single-layer graphene," *Nano Lett.*, vol. 8, no. 3, pp. 902–907, Feb. 2008.

[7] J. Moser, A. Barreiro, and A. Bachtold, "Current-induced cleaning of graphene," *Appl. Phys. Lett.*, vol. 91, no. 16, p. 163513, Sep. 2007.

[8] W. S. Hummers, Jr., and R. E. Offeman, "Preparation of graphitic oxide," *J. Amer. Chem. Soc.*, vol. 80, no. 6, p. 1339, Jan. 1958.

[9] L. Staudenmaier, "Verfahren zur Darstellung der Graphitsäure," *Berichte der deutschen chemischen Gesellschaft*, vol. 31, no. 2, pp. 1481–1487, May/Aug. 1898.

[10] L. J. Cote, J. Kim, C. V. Tung, J. Luo, F. Kim, and J. Huang, "Graphene oxide as surfactant sheets," *Pure Appl. Chem.*, vol. 83, no. 1, pp. 95–110, Dec. 2010.

[11] R. H. Fowler and L. Nordheim, "Electron emission in intense electric fields," *Proc. R. Soc. Lond. A, Math. Phys. Sci.*, vol. 119, no. 781, pp. 173–181, May 1928.

[12] A. H. Castro Neto, F. Guinea, N. M. R. Peres, K. S. Novoselov, and A. K. Geim, "The electronic properties of graphene," *Rev. Modern Phys.*, vol. 81, no. 1, pp. 109–162, Feb. 2009.

[13] Y.-T. Chang, J.-S. Wang, S.-Y. Su, Y.-J. Chih, and C.-H. Chen, "Field emission electrons of single- and double-layer graphene by using chemical vapor deposition," in *Proc. 9th Int. Conf. Opt.-Photon. Design Fabrication Itabashi Culture Hall*, Tokyo, Japan, Feb. 2014, pp. 1–2.

[14] G. Ko, Y. Jung, K.-Y. Lee, K. Lee, and J. Kim, "Improved sorption characteristics of NH_3 molecules on the solution-processed graphene sheets," *J. Crystal Growth*, vol. 326, no. 1, pp. 208–211, Jul. 2011.

[15] Y.-T. Chang, Y.-J. Chih, B.-S. Lin, and C. Hu Chen, "Field emission of electrochemical graphene oxide," in *Proc. 4th Int. Symp. Next-Genera. Electron. (ISNE)*, Taipei, Taiwan, May 2015, pp. 1-4.

[16] Y.-T. Chang, C.-T. Chang, G.-S. Li, and T.-S. Horng, "Reducing electrochemical exfoliated graphene defects by changing the insert voltage and electrolyte composition," in *Proc. 5th Int. Symp. Next-Generat. Electron.*, Hsinchu, Taiwan, May 2016, pp. 1–2.

[17] C.-Y. Su, A.-Y. Lu, Y. Xu, F.-R. Chen, N. A. Khlobystov, and L.-J. Li, "High-Quality thin graphene films from fast electrochemical exfoliation," *ACS Nano*, vol. 5, no. 3, pp. 2332–2339, Feb. 2011.

[18] T. Theres Baby and S. Ramaprabhu, "Cold field emission from hydrogen exfoliated graphene composites," *Appl. Phys. Lett.*, vol. 98, no. 18, p. 183111, Apr. 2011.

[19] K. Urbas, *et al.*, "Chemical and magnetic functionalization of graphene oxide as a route to enhance its biocompatibility," *Nanosc. Res. Lett.*, vol. 9, no. 1, p. 656, Sep. 2014.

[20] C.-C. Kuo and C.-H. Chen, "Graphene thickness-controlled photocatalysis and surface enhanced Raman scattering," *Nanosc.*, vol. 6, no. 21, pp. 12805–12813, Aug. 2014.

[21] W.-J. Lan and C.-H. Chen, "Hybridization of graphene in 3D complex nanovoids: Synergistic nanocomposites for electrocatalytic reduction of hydrogen peroxide," *Electrochim. Acta*, vol. 180, pp. 1014–1022, Oct. 2015.

[22] H.-L. Guo, X.-F. Wang, Q.-Y. Qian, F.-B. Wang, and X.-H. Xia, "A green approach to the synthesis of graphene nanosheets," *ACS Nano*, vol. 3, no. 9, pp. 2633–2659, Aug. 2009.

[23] S. Yong Toh, K. S. Loh, S. K. Kamarudin, and W. R. W. Daud, "Graphene production via electrochemical reduction of graphene oxide: Synthesis and characterisation," *Chem. Eng. J.*, vol. 251, pp. 422–434, Sep. 2014.

[24] D. C. Marcano *et al.*, "Improved synthesis of graphene oxide," *ACS Nano*, vol. 4, no. 8, pp. 4806–4814, Jul. 2010.

[25] G. Shao, Y. Lu, F. Wu, C. Yang, F. Zeng, and Q. Wu, "Graphene oxide: The mechanisms of oxidation and exfoliation," *J. Mater. Sci.*, vol. 47, no. 10, pp. 4400–4409, May 2012.

[26] C. D. Wanger, W. M. Riggs, L. E. Davis, J. F. Moulder, and G. E. Muilenberg, *Handbook of X-Ray Photoelectron Spectroscopy*. Eden Prairie, MN, USA: Perkin-Elmer Corp., 1979, pp. 12–30.

[27] J. Yan *et al.*, "Electrochemical properties of graphene nanosheet/carbon black composites as electrodes for supercapacitors," *Carbon*, vol. 48, no. 6, pp. 1731–1737, May 2010.

[28] B. Xu, *et al.*, "What is the choice for supercapacitors: Graphene or graphene oxide?" *Energy Environ. Sci.*, vol. 4, no. 8, pp. 2826–2830, Jun. 2011.

[29] S. Stankovich, *et al.*, "Synthesis of graphene-based nanosheets via chemical reduction of exfoliated graphite oxide," *Carbon*, vol. 45, no. 7, pp. 1558–1565, Jun. 2007.

[30] M.-H. Park, T.-H. Kim, and C.-W. Yang, "Thickness contrast of few-layered graphene in SEM," *Guidelines Special Issues*, vol. 44, nos. 11–12, pp. 1538–1541, Dec. 2012.

[31] Y. Li, M. V. Zijll, S. Chiang, and N. Pan, "KOH modified graphene nanosheets for supercapacitor electrodes," *J. Power Sour.*, vol. 196, no. 14, pp. 6003–6006, Jul. 2011.

Authors' photographs and biographies not available at the time of publication.